Self-Assembled Multilayers of 4,4‘-Dimercaptobiphenyl Formed by Cu(II)-Catalyzed Oxidation

ARTICLE *in* LANGMUIR · AUGUST 2002

Impact Factor: 4.46 · DOI: 10.1021/la020084k

7 AUTHORS, INCLUDING:

Jayne C Garno
Louisiana State University
88 PUBLICATIONS **1,682** CITATIONS

SEE PROFILE

Abraham Ulman
Polytechnic Institute of New York University
92 PUBLICATIONS **11,836** CITATIONS

SEE PROFILE

Self-Assembled Multilayers of 4,4′-Dimercaptobiphenyl Formed by Cu(II)-Catalyzed Oxidation

Tina Louise Brower,[†] Jayne C. Garno,[‡] Abraham Ulman,*[,†] Gang-yu Liu,[‡] Chun Yan,[§] Armin Gölzhäuser,[§] and Michael Grunze[§]

Department of Chemical Engineering, Chemistry, and Materials Science, and NSF MRSEC for Polymers at Engineered Interfaces, Polytechnic University, Six Metrotech Center, Brooklyn, New York 11201, Department of Chemistry, Wayne State University, Detroit, Michigan 48202, and Angewandte Physikalische Chemie, Universität Heidelberg, 69120 Heidelberg, Germany

Received January 25, 2002. In Final Form: April 23, 2002

Self-assembled multilayers were prepared by alternate deposition of 4,4′-dimercaptobiphenyl (DMBP) and copper(II) ions onto planar Au(111) substrates. The multilayers were characterized by ellipsometry, external reflectance Fourier transform infrared spectroscopy (ER-FTIR), X-ray photoelectron spectroscopy (XPS), and atomic force microscopy (AFM). Ellipsometry and ER-FTIR results show a linear relationship between the number of layers and the integral area of absorption characteristic of vibrational modes assigned to the biphenyl moieties. XPS data suggest that the copper is present in the +1 and +2 oxidation states in bulk material made by the reaction of DMBP and Cu(II) ions in solution, and only in the +1 state in multilayer films. XPS results also indicate a linear relationship between the number of DMBP layers and film thickness. AFM studies provided details about the surface morphology. In addition, thickness was measured precisely via nanoshaving and nanografting techniques. On the basis of the combination of these techniques, it is proposed that the DMBP multilayer system is formed by interlayer disulfide linkages.

Introduction

Organic thin films have attracted considerable attention for both fundamental and potential application reasons. The fundamental interest stems from the need to understand and control structures at the molecular level and the interfacial interactions that lead to their formation. The practical consequences of achieving such control include surface-dependent technologies such as chemical sensing[1−3] and synthetic light harvesting.[4] Molecular self-assembly is a simple method for preparing organic films with controlled thickness and surface behavior, and thus has become the preferred route for the preparation of molecularly engineered systems.

The development of organized molecular assemblies at interfaces started with Langmuir−Blodgett films[5] and proceeded through alkyltrichlorosilane multilayers,[6−9] metal bisphosphonate multilayers,[10,11] and more recently other organometallic systems.[12,13] Organometallic multilayers of ω-mercaptoalkanoic acids [$HS(CH_2)_nCOOH$], based on the interaction of Cu(II) ions with carboxylic acids and thiols, were reported.[14] There, the bolaamphiphiles were attached to the gold substrate via their thiol functionality, and the resulting self-assembled monolayer (SAM) was exposed to a solution of Cu(II) ions to form the corresponding copper carboxylate surface layer. When this layer was exposed to a solution of the bolaamphiphile, a second layer was attached through the thiol functionality. Repeating this process provided multilayer films. The experimental data suggested that during assembly the Cu(II) is reduced to Cu(I), and disulfide moieties are formed.[15,16] Similarly, Bard and co-workers reported the self-assembly of multilayers on gold using ω-mercaptoalkanethiols [$HS(CH_2)_nSH$] and Cu(II) ions. X-ray photoelectron spectroscopic (XPS) data confirmed a Cu(I) oxidation state and the formation of a multilayer with intralayer disulfide bonds.[17]

Recently, SAMs of aromatic rigid thiols on gold surfaces[18] attracted attention because of their potential as molecular wires[19] and electron beam resists,[20,21] and their

* Corresponding author. Telephone: (718) 260-3119. Fax: (718) 260-3125. E-fax: (810) 277-6217. E-mail: aulman@duke.poly.edu.
[†] Polytechnic University.
[‡] Wayne State University.
[§] Universität Heidelberg.

(1) Sun, L.; Kepley, L. J.; Crooks, R. M. *Langmuir* **1992**, *8*, 2101.
(2) Yang, H. C.; Dermody, D. L.; Xu, C.; Ricco, A. J.; Crooks, R. M. *Langmuir* **1996**, *12*, 726.
(3) Wells, M.; Dermody, D. L.; Yang, H. C.; Kim, T.; Ricco, A. J.; Crooks, R. M. *Langmuir* **1996**, *12*, 1989.
(4) Kaschak, D. M.; Mallouk, T. E. *J. Am. Chem. Soc.* **1996**, *118*, 4222.
(5) (a) Blodgett, K. *J. Am. Chem. Soc.* **1935**, *57*, 1007. (b) Blodgett, K. *Phys. Rev.* **1937**, *51*, 964. (c) Gaines Jr., G. L. *Insoluble Monolayers at Liquid−Gas Interfaces;* Interscience: New York, 1966. (d) Ulman, A. *An Introduction to Ultrathin Organic Films;* Academic Press: Boston, 1991.
(6) Tillman, N.; Ulman, A.; Penner, T. L. *Langmuir* **1989**, *5*, 101.
(7) Heid, S.; Effenberger, F.; Bierbaum, K.; Grunze, M. *Langmuir* **1996**, *12*, 2118.
(8) Kato, S.; Pac, C. *Langmuir* **1998**, *14*, 2372.
(9) Li, D. Q.; Ratner, M. A.; Marks, T. J.; Zhang, C. H.; Yang, J.; Wong, G. K. *J. Am. Chem. Soc.* **1990**, *112*, 7389.
(10) Lee, H.; Kepley, L. J.; Hong, H.-G.; Mallouk, T. E. *J. Am. Chem. Soc.* **1988**, *110*, 618.
(11) Katz, H. E.; Scheller, R. G.; Putvinski, T. M.; Schilling, M. L.; Wilson, W. L.; Chidsey, C. E. D. *Science* **1991**, *254*, 1485.
(12) Ansell, M. A.; Cogan, E. B.; Page, C. J. *Langmuir* **2000**, *16*, 1172.
(13) Hatzor, A.; Moav, T.; Cohen, H.; Matlis, S.; Libman, J.; Vaskevich, A.; Shanzer, A.; Rubinstein, I. *J. Am. Chem. Soc.* **1998**, *120*, 13469.
(14) Evans, S. D.; Ulman, A.; Goppert-Berarducciand, K. E.; Gerenser, L. J. *J. Am. Chem. Soc.* **1991**, *113*, 5866.
(15) Evans, S. D.; Freeman, T. L.; Flynn, D. N.; Ulman, A. *Thin Solid Films* **1994**, *244*, 778.
(16) Freeman, T. L.; Evans, S. D.; Ulman, A. *Thin Solid Films* **1994**, *244*, 784.
(17) Brust, M.; Blass, P. M.; Bard, A. J. *Langmuir* **1997**, *13*, 5602.
(18) Sabatani, E.; Cohen-Boulakia, J.; Bruening, M.; Rubinstein, I. *Langmuir* **1993**, *9*, 2974.
(19) *Nanostructure Physics and Fabrication;* Reed, M. A., Kirk, W. P., Eds.; Academic Press: New York, 1992
(20) Geyer, W.; Stadler, V.; Eck, W.; Zharnikov, M.; Gölzhäuser, A.; Grunze, M. *Appl. Phys. Lett.* **1999**, 75, 2401.

10.1021/la020084k CCC: $22.00
Published on Web 07/13/2002

ability to form stable model surfaces.[22] Beyond their rigidity, one advantage of these aromatic thiols is the conjugation between the adsorbing thiolate and the 4′-substituent. This was demonstrated when the adsorption kinetics[23] and the composition of mixed SAMs[24,25] changed as the electron donor/acceptor of the substituent at the 4′-position changed. The conjugation between substituents at the 4- and 4′-positions results from the apparent coplanarity of the biphenyl system in the two-dimensional assembly that can be inferred from the coplanarity in the molecular crystal.[26]

Sita and Tour have prepared phenylacetylene oligomers with the aim of developing molecular conductors by extending the length of the conjugated thiol molecule. This elegant multistep, but tedious, synthesis makes the preparation of very long molecules increasingly more difficult, especially since the solubility of these molecules in organic solvents, when unsubstituted, decreases with increasing molecular length. Thus, another strategy for the preparation of molecular conductors should be considered if one wants to develop molecular-based devices. We envisage that long molecular conductors may be prepared, in principle, via interlayer conjugation. Such conjugation can be realized by using transition metal ions to connect conjugated molecules bearing the proper functionalities at their α,ω-positions. In this paper we report the formation and structure of self-assembled multilayers using 4,4′-dimercaptobiphenyl (DMBP) and Cu(II) ions. Work is in progress to establish electron-transfer rates through these systems.

Experimental Section

Materials. The preparation of DMBP is described elsewhere.[27] Copper(II) perchlorate hexahydrate ($Cu(ClO_4)_2 \cdot 6H_2O$), 98%, was obtained from Aldrich and used as received. Docosanethiol was prepared from the corresponding bromide.[28] Dodecanethiol ($CH_3(CH_2)_{11}SH$), 98%, was obtained from Aldrich and used as received.

Substrate Preparation. Details of the thermal evaporation of gold on glass have been published elsewhere.[25] The reproducible optical constants for the gold substrates prepared according to this procedure are $N_S = 0.186 \pm 0.01$ and $K_S = 3.400 \pm 0.05$. These substrates were used for ellipsometry and Fourier transform infrared spectroscopic experiments. Substrates used for XPS measurements were prepared, according to a procedure by Yan and co-workers,[29] by evaporating a 100 nm gold film on a 1.0 nm titanium adhesion interlayer on polished silicon wafers. Ultraflat gold substrates were prepared following Wagner and co-workers.[30] This procedure produced samples with flat Au(111) terraces as large as 300 × 300 nm. The resulting gold surfaces have a mean roughness of 0.2−0.5 nm according to AFM measurements.

Multilayer Synthesis. Multilayer films were constructed by first immersing a freshly prepared gold substrate into a 1 μM solution of DMBP in ethanol for approximately 3 h, under nitrogen. SAM formation was monitored ex situ by ellipsometry and external reflectance Fourier transform infrared (ER-FTIR) spectroscopy. After monolayer formation was complete, the substrates were thoroughly washed with fresh ethanol and immediately exposed to a 50 mM $Cu(ClO_4)_2 \cdot 6H_2O$ solution in ethanol for 3 h. After a thorough rinsing with water and ethanol, and drying with a jet of nitrogen, subsequent layers were made by successive exposure to DMBP and $Cu(ClO_4)_2 \cdot 6H_2O$ solutions.

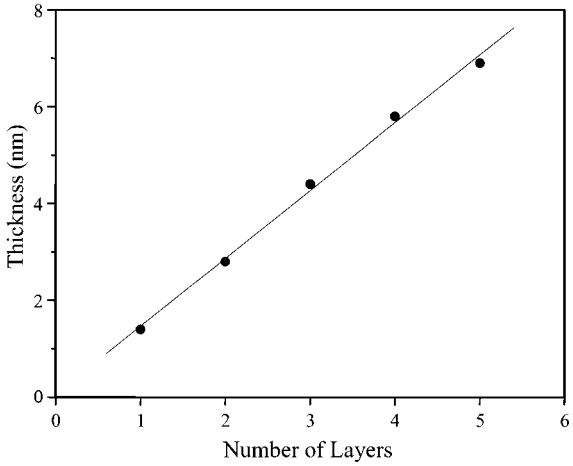

Figure 1. Ellipsometric thickness data for multilayer growth. The measurements were taken after the addition of organic layer. The adsorption time was 3 h for both the organic and ionic layers.

Ellipsometry Measurements. Layer thickness was estimated by ellipsometry using a Rudolph Research AutoEL ellipsometer (He−Ne laser, angle of incidence 70°). Measurements of three separate points were carried out on each sample, using an assumed refractive index of 1.462.

Fourier Transform Infrared Spectroscopy (FTIR). The FTIR spectra were obtained using a Nicolet MAGNA-IR 760 spectrometer equipped with a nitrogen-cooled MCT-A detector.[25] For each sample, 2500 scans were collected, with a resolution of 1 cm^{-1}. The spectra of bulk samples were collected in a transmission mode (200 scans, 1 cm^{-1} resolution).

Atomic Force Microscopy (AFM). A home-built scanner with optical beam deflection configuration was used for AFM studies. The electronic controllers and software were commercial units from RHK Technology, Inc. (Troy, MI). Images were acquired in ethanol using contact mode imaging. The AFM scanner was calibrated using both mica(0001) and Au(111) surfaces. Commercially available Si_3N_4 cantilevers, with force constants of 0.1 N/m (ThermoMicroscopes, Sunnyvale, CA), were used for imaging. Typically, the imaging force was 0.1 nN.

X-ray Photoelectron Spectroscopy (XPS). Spectra were recorded with a Leybold LH-12 equipped with Mg Kα ($h\nu = 1253.6$ eV) and Al Kα ($h\nu = 1486.6$ eV) sources, typically operated at 240 W. An aluminum anode was chosen in this study. Spectra (∼1.0 eV experimental resolution) were taken at normal emission using analyzer pass energies of 100 and 24 eV for the survey and detailed spectra, respectively. The pressure during measurements was $\leq 4 \times 10^{-9}$ mbar. Prior to peak fitting, a background subtraction was performed by the Shirley method. The energy scale was referenced to the Au $4f_{7/2}$ resonance at 84.0 eV. XPS measurements of the bulk

Results

We first reacted DMBP with $Cu(ClO_4)_2 \cdot 6H_2O$ to examine the reaction of the thiophenol groups with Cu(II) ions. The details of this experiment are given in the Supporting Information. The key points that are relevant to the discussion here are (1) the absence of an SH stretching band (2500−3000 cm^{-1}) in the spectrum of the DMBP−Cu bulk material, indicating a complete reaction of the SH groups; (2) the absence of any perchlorate vibrations,

(21) Gölzhäuser, A.; Geyer, W.; Stadler, V.; Eck, W.; Grunze, M.; Edinger, K.; Weimann, Th.; Hinze, P. *J. Vac. Sci. Technol. B* **2000**, 18, 3414.
(22) Kang, J. F.; Jordan, R.; Ulman, A. *Langmuir* **1998**, *14*, 3983
(23) Liao, S.; Ulman, A.; Shnidman, Y. *J. Am. Chem. Soc.* **2000**, *122*, 3688.
(24) Kang, J. F.; Liao, S.; Jordan, R.; Ulman, A. *J. Am. Chem. Soc.* **1998**, *120*, 9662.
(25) Kang, J. F.; Ulman, A.; Liao, S.; Jordan, R. *Langmuir* **1999**, *15*, 2095.
(26) von Laue, L.; Ermark, F.; Gölzhäuser, A.; Haeberlen, U.; Häcker, U. *J. Phys.: Condens. Matter* **1996**, *8*, 3977.
(27) Kang, J. F.; Ulman, A.; Liao, S.; Jordan, R.; Yang, G.; Liu, G.-y.; *Langmuir* **2001**, *17*, 95.
(28) Bain, C. D.; Troughton, E. B.; Yao, T.-T.; Evall, J.; Whitesides, G. M. *J. Am. Chem. Soc.* **1989**, *111*, 321.
(29) Yan, C.; Gölzhäuser, A.; Grunze, M.; Woell, Ch. *Langmuir* **1999**, *15*, 2414.
(30) Wagner, P.; Hegner, M.; Guntherodt, H.-J.; Semenza, G. *Langmuir* **1995**, *11*, 3867.

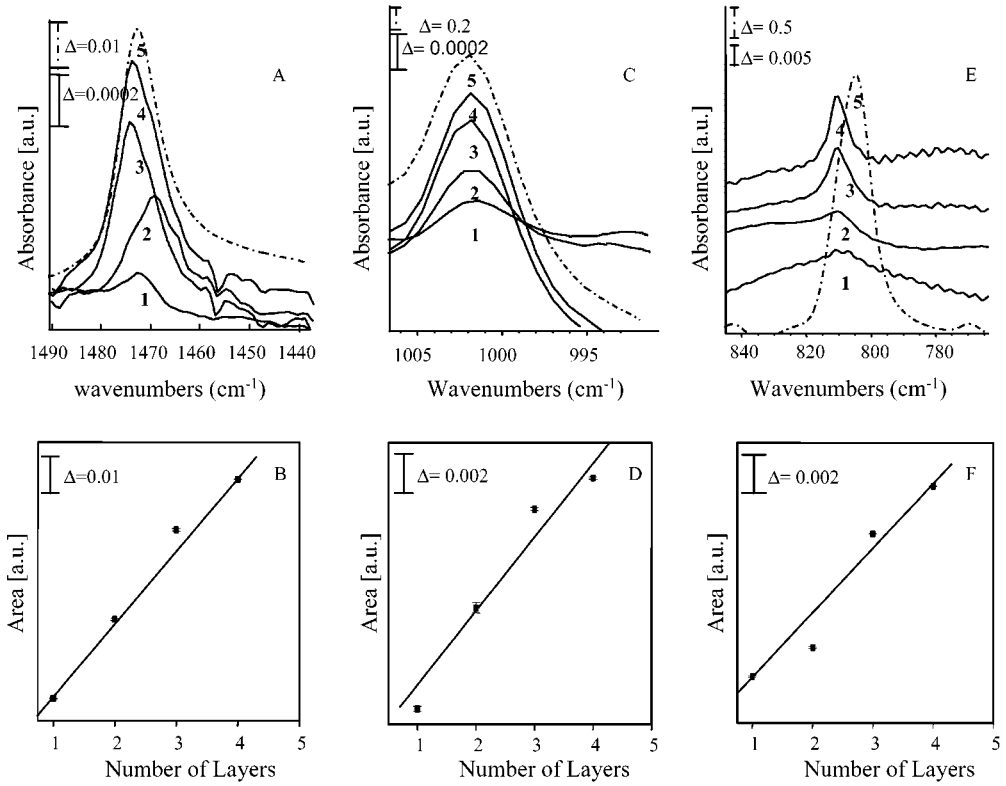

Figure 2. Comparison of transmission and external reflectance infrared spectra of the adsorbed DMBP monolayer and multilayers. (A), (C), and (E) are the bands for three aromatic vibrations of a tetralayer. 1, 2, 3, and 4 correspond to a monolayer through tetralayer, respectively. (B), (D), and (F) correspond to integral areas of absorbances. 5 corresponds to the isotropic DMBP−Cu system.

suggesting that charge neutralization for copper ions is provided by thiolate ions in the material; (3) the formation of a sulfur intermediate species such as metal-deficient sulfides and disulfides;[31] and (4) the presence of both Cu(I) and Cu(II) ions in the material.

Multilayers were prepared by the alternate exposure of Au(111) substrates to DMBP and Cu(II) ions. SAM growth was monitored by ellipsometry, and measurements were taken after the adsorption of the DMBP. Figure 1 shows a linear relationship between ellipsometric thickness and the number of adsorbed layers. The slope of the line is 1.4 nm.

External reflectance Fourier transform infrared (ER-FTIR) spectroscopy is not only a tool used to confirm the presence of specific molecules at the surface, but is also valuable for investigating the structural evolution of the SAM structure. The ER-FTIR spectra of three aromatic bands along with their areas are presented in Figure 2. The corresponding band for the isotropic DMBP−Cu bulk material has been included for comparison. We first consider the band that is assigned to a stretching mode of the aromatic ring, which is present around 1472 cm^{-1} in the isotropic spectrum.[32] A negative shift in this peak is indicative of a tilt of the long axis of the benzene ring toward the Au surface. This tilt would require the benzene to occupy a larger cross-sectional area, and therefore might diminish intermolecular attractions between neighboring phenyl rings ref 33. The loss of such interactions would result in a poorly defined monolayer and subsequent layers. The figures include a monolayer through a tetralayer labeled 1 through 4. The isotropic spectrum, labeled 5, has a band maximum at 1475.8 cm^{-1}. The band maxima of the first and second layers are shifted by only 6 and 2 cm^{-1}, respectively. The third and fourth layers both have a band maximum at 1474.8 cm^{-1}, which is different from the bulk spectrum by only 1 cm^{-1}. Furthermore, the area under this band increases linearly with the increasing number of layers in the film.

The integrated area of the band around 1000 cm^{-1}, common to all 4′-substituted 4-mercaptobiphenyl SAMs,[27] which is assigned to the C−C−C parallel bending of the phenyl moiety, also increases linearly with the number of layers in the film. In addition, a band for out-of-plane wagging (at 817 cm^{-1}) is observed. This band should not be IR active in an ER-FTIR experiment for SAMs with biphenyl moieties that are perpendicular to the surface, because of surface selection rules. However, in some biphenyl thiolate SAMs on gold it is observed.[27] When compared to the isotropic spectrum, the intensity of this peak is negligible and suggests a small molecular tilt with respect to the surface normal.[31] While it is not possible to exert an exact tilt angle from the present measurements, infrared spectra of numerous biphenyl thiolate SAMs,[27] as well as diffractions studies,[32] suggest a tilt angle of ≤15°. The integrated area under the 817 cm^{-1} band increases with the increasing number of layers. The linear relationship suggests that the tilt angle of the biphenyl moieties does not increase, which implies no development of disorder with the increasing layer number.

The XPS survey spectrum of a multilayer sample containing three layers showed signals for gold, carbon, copper, sulfur, and a little oxygen, possibly from contaminants. Figure 3A presents a detailed spectrum of the sulfur peak for the trilayer sample after treatment with the $Cu(ClO_4)_2 \cdot 6H_2O$ solution. Two S 2p (1/2, 3/2) doublets are visible after peak deconvolution, corresponding to two atomic species, one at a S $2p_{3/2}$ binding energy of 162.0 eV,

(31) Zachwieja, J. B.; et al. *J. Colloid Interface Sci.* **1990**, *132*, 462.
(32) Leung, T. Y. B.; Schwartz, P.; Scoles, G.; Schreiber, F.; Ulman, A. *Surf. Sci.* **2000**, *458*, 34.

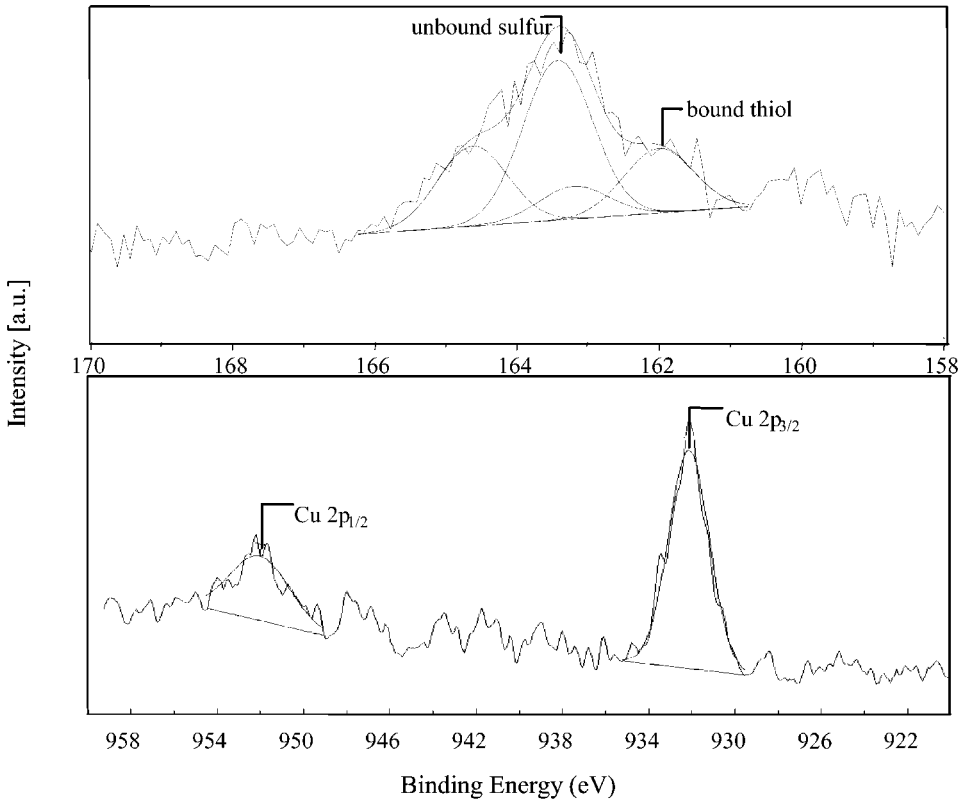

Figure 3. XP spectra of DMBP−Cu multilayer film: (A, top) S 2p spectrum of a trilayer after treatment with copper(II) perchlorate hexahydrate. The peaks were fitted using two S 2p doublets assigned to bound and unbound thiolate. (B, bottom) Cu 2p spectra of a trilayer after treatment with copper(II) perchlorate hexahydrate. The binding energies correspond to Cu(I); the presence of Cu(II) can be excluded.

Table 1. Percentages of Sulfur Species for Multilayers

layer	thiolate (%)	thiol, disulfide (%)
monolayer	38	62
monolayer with copper	45	55
bilayer	24	76
bilayer with copper	32	68
trilayer	29	71
trilayer with copper	35	65
tetralayer	21	79
tetralayer with copper	25	75
pentalayer	0	100

which can be assigned to thiolate species, and another at 163.1 eV, which can be assigned to neutral sulfur species (e.g., disulfide). Interestingly, the intensity of the thiolate peak increases when copper is attached to the first layer, suggesting that the SH is deprotonated and the thiolate forms a bond with a copper ion. Once a second mercaptobiphenyl is adsorbed, the intensity of the thiolate decreases, suggesting that thiolates were consumed, which can be rationalized by the formation of S−S moieties that connect the first and the second layers. The signal of the thiolate sulfur decreases with the increasing number of layers, and disappears after five layers were assembled, most likely due to attenuation of the Au−S thiolate. (See Table 1.) We shall return to this point in the discussion section of this paper.

The detailed spectrum of the Cu region is given in Figure 3B. The binding energy of Cu $2p_{3/2}$ is 932 eV and the kinetic energy of copper Auger line Cu(L_3VV) is 918.1 eV, corresponding to Cu(I) state, thus excluding the presence of Cu(II). The concentration of Cu(I) shows an insignificant increase with the increasing number of layers. The thickness of the copper-terminated layers was estimated by using the attenuation of Au 4f peaks. If these data are fitted by linear regression, we find a straight line with a slope of 0.8 nm and a *y*-intercept of 1.2 nm, which corresponds to the thickness of a monolayer.

Two types of structural information are extracted from the AFM studies. First, AFM topography allows direct visualization of the surface morphology with high spatial resolution. Second, by combining AFM imaging and AFM-based lithography such as nanoshaving and nanografting, one could measure the thickness of the layers with angstrom precision.[33] In nanoshaving,[34] a high local pressure is applied by an AFM tip to the area of contact. This pressure causes high shear forces, and thus displaces SAM adsorbates during the scan. As a result, the bare substrate is exposed. The thickness of the films can be read directly from cursor profiles across the film and cleanly exposed substrate surfaces. Nanografting combines adsorbate displacement with the self-assembly of thiols on gold. In nanografting, the imaging medium contains a different thiol from the matrix. For the purpose of height measurement, we selected thiols of well-known structure. As the AFM tip scans at high force through the monolayer, the matrix molecules are removed and replaced by the new adsorbates from solution. The resulting nanografted structures are then characterized by imaging at low force. By comparing the height difference between the matrix and the nanopatterns of thiols with known height, the thickness of the matrix film can be extracted.

A monolayer, bilayer, and trilayer of DMBP were investigated using atomic force microscopy. The monolayer exhibits a clustered surface morphology, shown in Figure

(33) Tao, Y.-T.; Wu, C. C.; Eu; J.-W.; Ling-Lin, W. *Langmuir* **1997**, *13*, 4018.

(34) Xu, S.; Miller, S.; Laibinis, P. E.; Liu, G.-Y. *Langmuir* **1999**, *15*, 7244.

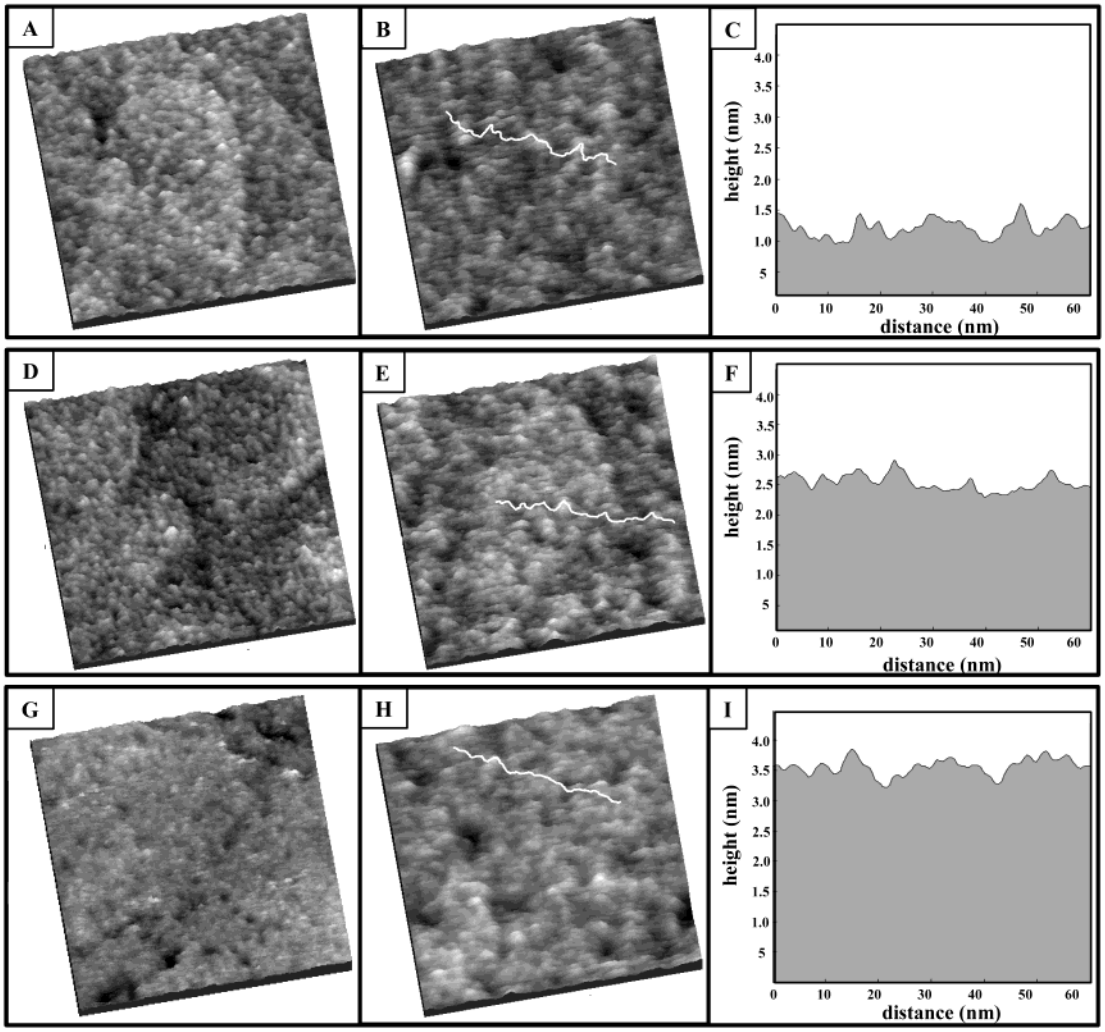

Figure 4. Comparison of the surface structure of monolayer, bilayer, and trilayer systems of DMBP. (A) AFM topographic image of a DMBP SAM on Au(111) for a 200 × 200 nm^2 scan area. (B) 100 × 100 nm^2 zoom-in view of the same layer. (C) Cursor profile in (B), indicating a surface roughness of 2−5 Å. (D) AFM topographic image (200 × 200 nm^2) of the surface of a double layer of DMBP. (E) 100 × 100 nm^2 scan of the same film. (F) Cursor profile in (E), showing a surface roughness of 2−5 Å. (G) 200 × 200 nm^2 scan of a trilayer of DMBP. (H) 100 × 100 nm^2 image of the same film. (I) The line in (H), indicating roughness of 3−6 Å for the trilayer film.

4A, with irregularly shaped islands covering the surface, measuring from 3 to 10 nm in width. Clearly resolved features of the underlying gold substrate are apparent, including gold terraces, with 2.8 ± 0.2 Å height, approximately 100 ± 150 nm in dimension. Zooming in to view the surface, in Figure 4B, reveals surface roughness more clearly. A cursor line across the image indicates the average roughness to be 0.2−0.5 nm as shown in the cursor measurement of Figure 4C. The surface structure for the bilayer is shown in Figure 4D,E. Images show that features of the gold substrate underneath the second layer can still be resolved, such as boundary domains and the edges of terrace steps. Similar to a monolayer, a random distribution of clusters of various sizes is viewed across the surface for the second layer. The clusters have widths that range from 4 to 10 nm for the bilayer. The surface roughness is, again, 0.2−0.5 nm as is profiled in the cursor plot of Figure 4F. In the next set of images, Figure 4G,H, a trilayer shows further surface changes. The underlying gold substrate is no longer clearly visible through the thicker multilayer. The width of the clusters has increased and ranges from 5 to 12 nm for a trilayer, and an increase in surface roughness is shown in the cursor profile of Figure 4I, now measuring from 0.3 to 0.6 nm.

The thickness of a DMBP SAM is 1.01 ± 0.22 nm, measured by nanoshaving, as shown in Figure 5. The *x*-offset correction introduced an artifact into the processed topography image, which displays bright bands at the sides of the square hole. The matrix is homogeneous in height surrounding the nanoshaved area. Some of the displaced DMBP molecules were pushed to the edges of the hole and created a boundary that is taller than the matrix surrounding the square. Thus, to obtain an accurate depth measurement, the cursor was measured along the direction of the scan, referencing the outer areas of the matrix SAM and not the edges. The cursor measurements were made before processing the image, and the example shown represents a single line measurement that is typical of several cursor profiles.

DMBP molecules may remain or redeposit onto thiophilic gold substrates during nanoshaving, which becomes problematic with thicker layers (bi- or trilayer) of DMBP SAMs. We used nanografting as our tool to accurately measure the heights of multilayers. Topographic images acquired after nanografting various alkanethiols into a matrix SAM comprised of mono-, bi-, and trilayers of DMBP are shown successively in Figure 6A−F. In Figure 6A, a positive nanopattern of dodecanethiol is shown to

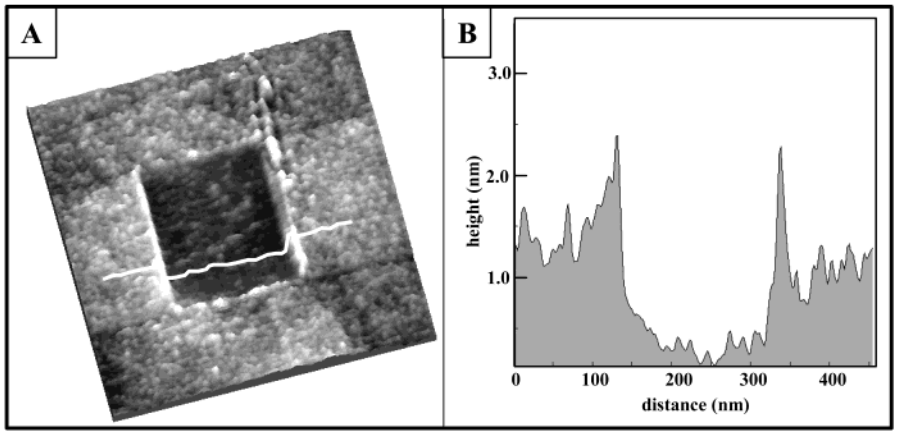

Figure 5. Thickness of a DMBP monolayer measured using nanoshaving. (A) 500 × 500 nm^2 topographic scan in which 200 × 200 nm^2 of the monolayer is displaced using nanoshaving. This image was processed by plane subtraction, *x*-offset correction, and smoothing. (B) Cursor profile as indicated in (A), revealing a depth of 1.01 ± 0.22 nm. The materials at the edge of the square are likely molecules displaced during fabrication.

be 0.50 ± 0.18 nm taller than the matrix monolayer by the cursor measurement of Figure 6B. Since the known height of dodecanethiol is 1.54 nm, comparison gives the height of the DMBP monolayer of 1.04 nm ± 0.18 nm, which is consistent with the nanoshaving measurement of Figure 5. Heights of the bilayer and trilayer samples were measured using docosanethiol SAM as the reference, which has a known height of 2.66 nm. As shown in Figure 6C, the resulting nanopattern has a positive height measuring 0.45 ± 0.25 nm above the matrix (Figure 6D). Therefore, the measured thickness of DMBP bilayer is 2.21 ± 0.25 nm, with the roughness included in the uncertainty. With a trilayer of DMBP as the matrix, a negative nanopattern was generated, as shown in Figure 6E. A cursor line, drawn vertically across the nanopattern (Figure 6F), shows a depth of 0.7 ± 0.25 nm. Adding this value to the 2.66 nm known height of docosanethiol gives a thickness of 3.36 ± 0.30 nm for the three-layer system.

The topographic images in Figure 6A,C allow simultaneous and direct views of the differences in surface morphology of the sulfur-terminated DMBP matrix layers from that of methyl-terminated alkanethiols of the nanopatterns. In contrast to the smooth, crystalline surface of densely packed *n*-alkanethiol SAMs within the nanopatterns, the surfaces of DMBP layers exhibit structural features of randomly distributed, irregularly shaped small domains. By comparing the surface topography of alkanethiol and DMBP layers side by side, we conclude that the roughness and domainlike features are the intrinsic characteristics of DMBP films.

Discussion

The exposure of a DMBP SAM to a solution of $Cu(ClO_4)_2 \cdot 6H_2O$ in ethanol results in formation of Cu(I) thiolate layer. FTIR and XPS data do not show any ClO_4^-, and taken together with the binding energy of Cu $2p_{3/2}$ at 932 eV and the kinetic energy of copper Auger line Cu(L_3VV) at 918.1 eV, it appears that a reduction of Cu(II) to Cu(I) has occurred. The problem is that there is no excess thiol in solution that could serve as a reducing agent, and reduction by the SAM thiols should result in the formation of intralayer S−S bond, which should be rejected given the S···S distance, which should be equal to that at the SAM−gold interface. The only possible reducing agent is the ethanol, and while we have not found a precedent for this reaction in solution, here the reaction occurs at the surface and is coupled with the formation of a strong S−Cu bond. Clearly, more work needs to be done to clarify this issue.

Ellipsometric and ER-FTIR data confirm that multilayers are formed by alternate exposure of a gold substrate to DMBP and $Cu(ClO_4)_2 \cdot 6H_2O$ solutions. The presence of an IR wag vibration band at 817 cm^{-1}, which is perpendicular to the biphenyl plane, is an indication of a molecular tilt, which is an agreement with helium and X-ray diffraction studies of 4′-methyl-4-mercaptobiphenyl,[35] NEXAFS studies of biphenylthiol,[20] as well as AFM studies of 4′-chloro-4-mercaptobiphenyl,[27] all suggesting that the biphenyl moieties in these SAMs on gold have a tilt angle of ≤15° with respect to the surface normal. This, however, might not be the tilt angle in the multilayer systems. The linear increase of the integral area of ER-FTIR data with the increasing number of layers suggests that the tilt remains approximately the same as the multilayers are formed.

The experimental data presented so far suggest that there can be two possible models for the multilayer structures (Figures 7 and 8). The first (disulfide model, Figure 7) proposes an interlayer S···S bonding as the driving force for multilayer formation. In the second (copper "sandwich" model, Figure 8), the DMBP units are connected by copper ions. In the following we discuss the different experimental data and present arguments suggesting that the first model is the most plausible one to describe the multilayer structure.

First Argument: *XPS data do not show a linear increase in copper concentration with increasing layer number.* If the sandwich model were correct, copper concentration should increase linearly with the increasing layer number. What is observed is that copper concentration increases insignificantly with increasing layer number. Moreover, XPS data show that only Cu(I) is present (Cu(II) is known to react with thiols to give disulfides and Cu(I)[36]) and the sandwich model requires that Cu(II) binds to two thiolates. If interlayer connection is provided by Cu(I), *intralayer* S−S bond formation must exist to support the exclusive presence of Cu(I), similar to the results of Bard and co-workers,[17] where in the multilayer the intralayer disulfides are still present and Cu(I) is sandwiched between two of the sulfur moieties in an alternating layer structure to preserve charge neutrality. This is

(35) Liu, G.-Y.; Xu, S.; Qian, Y. *Acc. Chem. Res.* **2000**, *33*, 457.
(36) Slagle, K. H.; Reid, E. E. *Ind. Eng. Chem.* **1932**, *24*, 448.

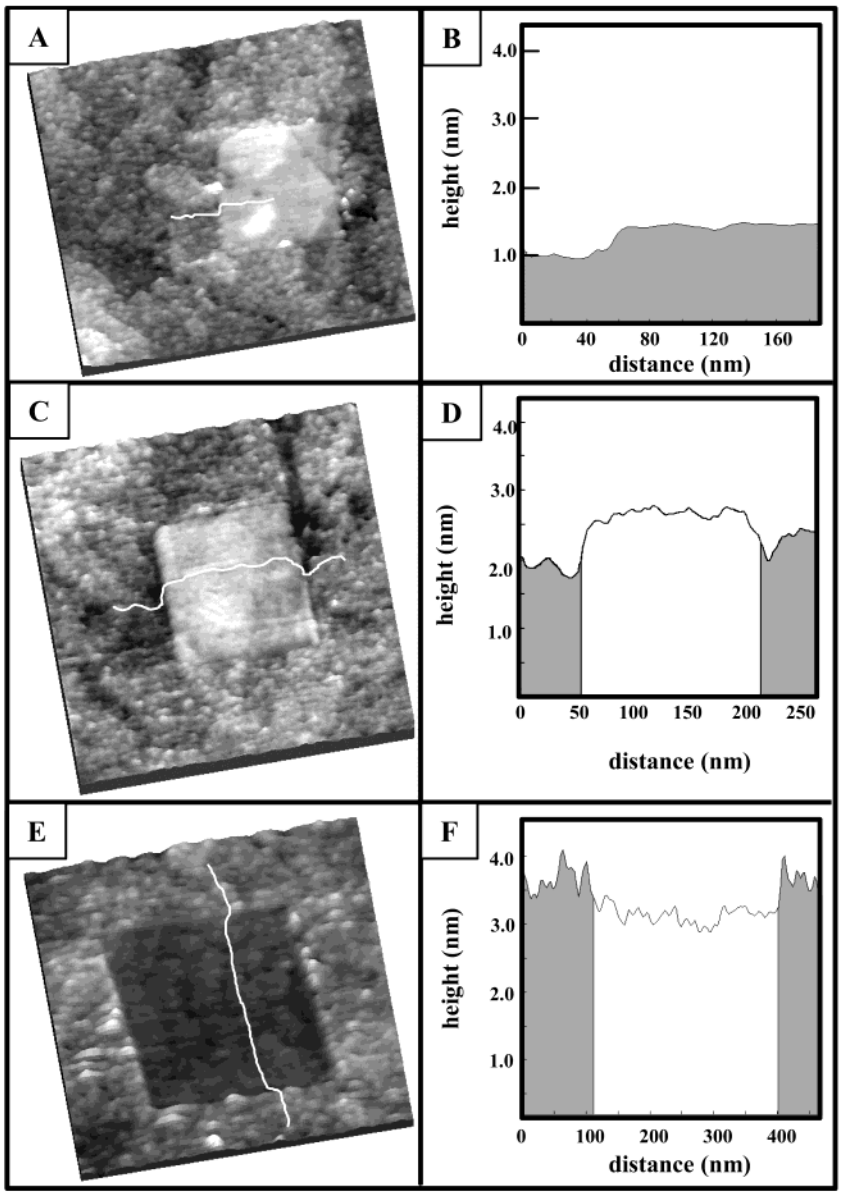

Figure 6. Height of three DMBP films as measured by nanografting. (A) 200 × 200 nm^2 square of dodecanethiol nanografted into a monolayer of DMBP. (B) Cursor line in (A), indicating that the alkanethiol is 0.50 ± 0.18 nm taller than the monolayer. Thus for the monolayer, the thickness is 1.04 ± 0.18 nm. (C) 600 × 600 nm^2 image of a bilayer within which a 150 × 150 nm^2 region of docosanethiol SAM was nanografted. (D) Cursor profile from (C) revealing that docosanethiol is 0.45 ± 0.25 nm taller than the DMBP bilayer; thus the bilayer has a thickness of 2.21 ± 0.25 nm. (E) 600 × 600 nm^2 topographic image of a trilayer within which a 300 × 300 nm^2 region of docosanethiol SAM was produced using nanografting. (F) Corresponding cursor profile indicating that the trilayer of DMBP is 0.70 ± 0.30 nm taller than the docosanethiol SAM, suggesting that the total thickness of the trilayer film is 3.36 ± 0.30 nm.

possible in the case of alkyl chains, due to the formation of a gauche conformational defect layer. However, in the case of DMBP a formation of intralayer S−S bonds is counterintuitive. This is because the S−S bond length in disulfides is ∼0.20 nm, and the minimum distance between the C−S carbons in adjacent phenyl rings is ∼0.30 nm. Therefore, if an intralayer S−S bond was formed, the distance between the two 4′-thiol groups would have been ∼0.76 nm, much larger that the 0.5 nm in a close packed epitaxial layer of thiolates on Au(111). Furthermore, in this case there would be a significant disruption of intermolecular interactions. Therefore, the sandwich model must be rejected on the basis of charge neutrality and XPS data.

Second Argument: *The concentration of thiolate sulfur does not increase with increasing number of layers.* A detailed study of the sulfur region of the monolayer and of subsequent multilayers shows that there are two sulfur species. The XPS data shows that while thiolate concentration in the monolayer is 38% (due to the Au−S bond formation), upon exposure to the $Cu(ClO_4)_2 \cdot 6H_2O$ solution its concentration increases to 45%, but decreases to 24% after exposure to DMBP solution, reflecting the attenuation of the adsorbing thiolate signal. With this attenuation in mind, any "sandwich" model requires the addition of a new thiolate layer with the addition of every DMBP layer. This is not observed, and the trend continues as the multilayers are formed, suggesting that the observed behavior is due to the formation of interlayer S−S bonds. The slight discrepancies between the "ideal" thiolate-to-disulfide ratios and the ones in Table 1 can be rationalized by the differences in the attenuation of the two sulfur species and the large error due to the high signal-to-noise ratio of the sulfur XP spectra.

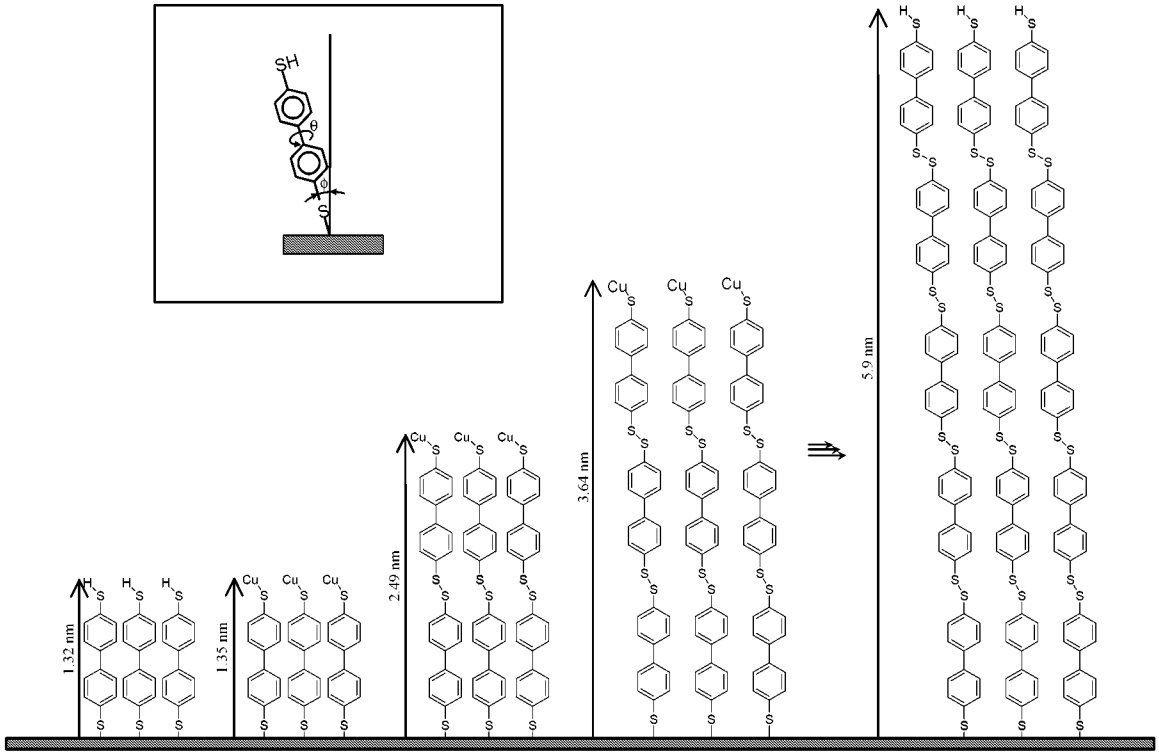

Figure 7. Proposed disulfide model of the multilayer. The inset shows the expected geometry of a SAM on Au(III) with a dihedral angle $\theta = 180°$ and a tilt with the surface normal, $\phi = 19°$. This model assumes the presence of Cu only at the top of the multilayer and corresponds to a Cu(I) oxidation state.

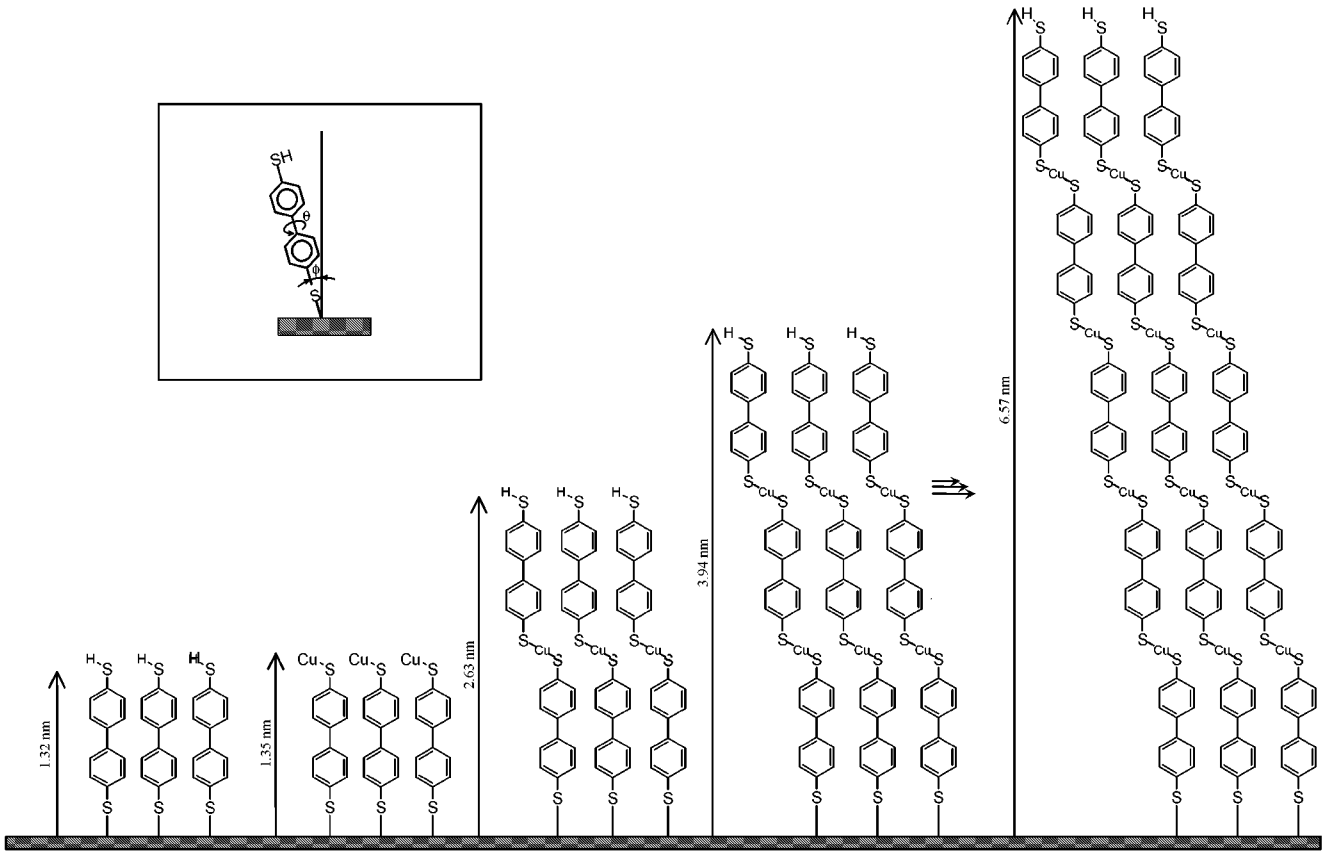

Figure 8. The copper sandwich model of the multilayer. This model assumes the formation of multilayers via the reduction of Cu(II) and the oxidation of the thiol to form a multilayer. The inset as in Figure 7.

Third Argument: *We need to point out that the thickness measurements in AFM reflect the true local thickness as alkanethiol SAMs with known structures were fabricated and compared with DMBP layers, side by side.*

Table 2. Thickness (nm) Measured by AFM for the Disulfide and Copper Sandwich Models[a]

layer	measured thickness (nm)	theoretical thickness (nm)	tilt angle (deg)
	Disulfide Model		
monolayer	1.01 ± 0.22 hole digging	1.12	25.6 ± 15
monolayer	1.04 ± 0.18 nanografting	1.12	21.8 ± 13
bilayer	2.21 ± 0.25 nanografting	2.29	15.2 ± 14.6
trilayer	3.36 ± 0.30 nanografting	3.44	12.3 ± 10.2
	Copper Sandwich Model		
monolayer	1.01 ± 0.22 hole digging	1.12	25.6 ± 16.1
monolayer	1.04 ± 0.18 nanografting	1.12	21.8 ± 13.6
bilayer	2.21 ± 0.25 nanografting	2.43	24.5 ± 11.4
trilayer	3.36 ± 0.30 nanografting	3.74	26.1 ± 9.2

[a] The table includes calculated tilt angles from AFM thickness.

XPS or ellipsometry, on the other hand, measure the spatially averaged thickness, which convolutes defects into the data. For the proposed model, thickness measured via AFM is used as the guide. The AFM studies employed here provided lateral and depth resolutions on a nanometer scale. The nanoshaving and nanografting techniques indicate a monolayer thickness of 1.04 ± 0.18 nm. This height does not support an interlayer S−S bond at the monolayer layer since this would require a height of twice that. Thus, there is no formation of multilayer in the absence of Cu(II) as was published for alkanethiols by Kohli and co-workers.[37] One could consider a mixture of monolayers and S···S double layers to reconcile the extra (28%) unbound sulfur species in the monolayer. (One expects a 1:1 ratio between thiolate and neutral, SH, sulfur in the monolayer.) However, the surface roughness is only 0.2−0.5 nm, which is consistent with that of the underlying gold.

Table 2 shows that when the two possible models are compared based on AFM and theoretical thickness, as determined by molecular modeling software, the agreement of experimental with theoretical thickness is better for the disulfide model. We calculated what tilt angle with respect to the surface normal would be required for the theoretical length to fit the actual thickness as measured by AFM. The tilt angles show a systematic decrease with increasing number of layers for the disulfide model. This can be justified on the basis of increasing packing and ordering as the number of layers increases.

To further examine the model of disulfide formation, we exposed a DMBP double layer to a 1 mM solution of 1,8-octanedithiol (ODT) for 16 h. XPS showed the expected ratio between aromatic and aliphatic carbons. We believe that, if the sandwich model were correct, there should have been at least some exchange due to the ODT concentration and the exposure time.[38]

Possible Mechanism. We now come to proposing a mechanism for the multilayer formation, taking into consideration all the data and arguments presented so far. It is important to note at the outset that surface reactions are not simple; for example, the exact nature of the reaction of thiols with gold surfaces to form dense thiolate SAMs is still not fully understood.

Cupric ions are known to catalyze oxidative coupling of terminal acetylenes to diacetylenes.[39] The mechanism of the Eglinton and Glazer reactions are thought initially to proceed by base removal of the terminal proton. Just how the carbanion becomes oxidized to the radical and what part the cuprous ion plays (other than forming the acetylide salt) are matters of considerable speculation,[40] and they depend on the oxidizing agent. We believe that the formation of the disulfide multilayers proceeds via an analogous mechanism, where the oxidizing agent is oxygen. Thus, although all reactions are carried out under nitrogen, there is enough oxygen present when we consider surface reactions. Therefore, any copper that was found by XPS inside the multilayers is probably due to unreacted copper(I) thiolate at different stages of the multilayer buildup. Interestingly, when mercuric ions are used, the multilayers have the sandwich-type structure. These results will be published shortly.

Conclusions

Self-assembled multilayers were been prepared by the alternate exposure of Au(111) substrates to DMBP and Cu(II) ions. Ellipsometry confirms the formation of multilayers, and ER-FTIR results show a linear relationship between the number of layers and the integral area of adsorption characteristic of vibrational modes assigned to the biphenyl moieties. XPS data show only Cu(I) peaks, thus excluding a structure of alternating DMBP and Cu(II) structure. Changes in the XPS thiolate peaks support the formation of DMBP multilayers via interlayer disulfide linkages, which are formed by the oxidation of Cu(II). The packing of DMBP is revealed in detail by AFM studies. In contrast to alkanethiol SAMs, which form a homogeneous morphology of closely packed, commensurate thiols on Au(111), the morphology of DMBP is less homogeneous, indicating that the molecules are less closely packed. With the treatment of copper perchlorate, multilayers form in a layer-by-layer fashion. The packing and morphology are maintained throughout the growth process.

Acknowledgment. This study was funded by the NSF through the MRSEC for Polymers at Engineered Interfaces and the GRT program. We thank Prof. Allen J. Bard for helpful discussion. G.-y.L. and J.C.G. acknowledge the

(37) Kohli, P.; Taylor, K. K.; Harris, J. J.; Blanchard, G. J. *J. Am. Chem. Soc.* **1998**, *120*, 11962.
(38) Brower, T.; Ulman, A. Manuscript in preparation.
(39) Campbell, I. D.; Eglinton, G. *Org. Synth.* **1965**, *45*, 39.
(40) Clifford, A. A.; Waters, W. A. *J. Chem. Soc.* **1963**, 3056.

initial participation of Yan Huang in this project, and thank Guohua Yang, Bill Price, and Sylvain Cruchon-Dupeyrat for helpful discussion. The AFM study was supported by NSF-IGERT-9879720. A.U. thanks the Alexander von Humboldt Foundation for supporting his stay at the University of Heidelberg.

Supporting Information Available: Text and figures discussing reaction between 4,4′-dimercaptobiphenyl and $Cu(ClO_4)_2 \cdot 6H_2O$ and FTIR and XP spectra. This material is available free of charge via the Internet at http://pubs.acs.org.

LA020084K